



Characterization of Elvitegravir and Its Related Impurities Using ESI–LC–MS, NMR Techniques, Method Development and Validation of Its Related Substances by HPLC Method

Sambandan Elumalai¹ · Sellappan Senthilkumar¹ · Mamidala Srikanth² · Venkata Bharat Nishtala³ · Kathavarayan Thenmozhi¹

Received: 2 August 2023 / Revised: 6 January 2024 / Accepted: 23 January 2024 / Published online: 22 February 2024
© The Author(s), under exclusive licence to Springer-Verlag GmbH Germany, part of Springer Nature 2024

Abstract

Elvitegravir (ETV), drug substance, and its eleven process-related impurities have been identified and their structural identification study has been carried out with the aid of ¹H, ¹³C NMR, and ESI–LC–MS spectroscopic techniques. Plausible fragments were also proposed for each impurity to ascertain its structure. Simple, facile, and selective, stability indicating, mass spectrometry compatible HPLC method has been developed and subsequently validated with the validation parameters of specificity, LOD, LOQ, precision at LOQ, linearity, accuracy at LOQ to 120% levels, method precision, intermediate precision studies, and solution stability has also been established. This method encompasses a simple gradient mode of separation with mobile phases—(A) 0.1% trifluoroacetic acid in water and (B) 0.1% trifluoroacetic acid in acetonitrile, the mass spectrometric compatible mobile phase has been chosen for the identification of known, unknown and degradation impurities. To assess the nature of each impurity, whether they are either process-related or degradation-induced, an intensive stress study has also been conducted. From this degradation assessment, all the impurities have been classified as process-related. Further, the assessment of three different manufacturers samples was also executed to show the method applicability and comparison of quality of the different manufacturers drug, and thus this method shall be engaged as a quality inferring tool for the marketed sample.

Keywords Elvitegravir · Process impurities · Characterization · HPLC method validation · Antiretroviral drug

Introduction

ETV belongs to a new class of antiretroviral drugs. This viral integrase inhibitor (INSTs) is used as an anti-HIV agent [1]. The pharmacokinetic activity of ETV has been studied by preventing the strand transfer step (viral genetic information integration) to the host cell DNA for viral replication

[2–4]. ETV is prone to biotransformation by hepatic CY3A4 cytochrome enzyme, thus preferred as a combination drug with Emtricitabine, Tenofovir disoproxil, or Cobicistat to enhance its antiretroviral activity [5, 6]. Presently, the drug is administered once daily as an oral dose intended only for adults [7]. ETV being an important investigational modern drug, diversified research has been conducted for its safety, efficacy, drug delivery, drug–drug interactions, [8–10] In-silico and QSAR evaluation of analogues, dosage details, [11–14], and even LC–MS/MS and UHPLC–MS/MS studies in the presence of other drugs [15–20]. However, information on ETV impurities, structural elucidation, their degradation information, and analytical methods for impurities separation in ETV are almost unavailable. Further, ETV is not official in any of the pharmacopeia monographs which includes USP, EP, BP, JP, and International pharmacopeias [21–23]. Thorough literature search has been carried out for the structural identification and characterization studies of few of the other drug compounds, all of them indicates that

✉ Venkata Bharat Nishtala
nvbharatnv@nita.ac.in

✉ Kathavarayan Thenmozhi
k.thenmozhi@vit.ac.in

¹ Department of Chemistry, School of Advance Sciences, Vellore Institute of Technology, Vellore 632014, India

² Department of Chemistry, National Institute of Technology Warangal, Warangal, Telangana 506004, India

³ Department of Chemistry, National Institute of Technology Agartala, Agartala, Tripura 799046, India

the impurities structural characterization studies have been carried out with the aid of LC–MS, NMR, UV, and IR techniques. The impurities separation and their purity estimation studies were conducted with the help of HPLC technique [24–27]. Therefore, in this research work, we have identified eleven process-related impurities of ETV drug. Their structural identification studies were carried out with the aid of ESI–LC–MS and NMR techniques. We also developed a stability indicating, simple and mass spectrometry compatible HPLC method to separate all these impurities. Three manufacturers samples were also tested to check purity of the ETV drug substance to forecast its quality.

Experimental methods

Materials

ETV sample was obtained from MSN laboratory, Hyderabad, India and ETV standard and its related impurities (HMB impurity, BQN impurity, Deschloro impurity, QAM impurity, DFB impurity, methyl ester impurity, 3-Cl-2,4-DFB impurity, Leucine impurity, 7-Ethoxy impurity, THP impurity and Dimer impurity) were synthesized in-house. Acetonitrile and water used were of HPLC gradient grade. All other chemicals and solvents used for chromatographic analysis were of analytical grade.

NMR Spectroscopy Instrumental Condition

The ^1H , and ^{13}C , NMR experiments were recorded using Bruker AV300/1 FT-NMR spectrometer (Bruker Corporation, Massachusetts, United States) equipped with a quad-probe capable of recording ^1H , ^{13}C , ^{19}F , and ^{31}P spectra and consisting Probe heads dual probe 5 mm DUX $^1\text{H}/^3\text{H}$ Z-GRD, broad-band probe (5 mm BBO- ^1H -D Z-GRD). The experiments were performed with DMSO- d_6 solvent for sample preparation. The ^1H NMR spectra were recorded with pulse program zg, ^1H , and ^{13}C chemical shift values are reported on δ scale in ppm relative to TMS as internal standards and DMSO- d_6 as solvent.

Mass Spectroscopy Instrumental Condition

Structural confirmation, mass screening, and fragmentation details of each impurity and ETV have been recorded using Agilent (1100 series) LC system interfaced to an ion trap mass analyzer (model G2445D SL) capable of mass range of 50–2200 m/z with adjustable scan speeds for normal, enhanced or maximum resolution and extended range 50–4000 m/z with normal resolution. Encompasses scan, Multiple Ion Monitoring (MRM), and MS (n) modes with

positive, negative, and alternating polarity ion detection facilities.

HPLC Instrumental Condition

HPLC investigation studies were conducted using Waters Alliance HPLC make (Model:2695) with PDA (Model:2998)/UV (Model:2489) detectors with Empower-2 chromatographic data system for chromatographic data acquisition. Impurities separation was achieved with Peerless Basic C18 HPLC column of length 250 mm, width of 4.6 mm, and particle size of 3 μm . Binary mixtures of mobile phases (mobile phase A: 0.1% trifluoroacetic acid in water (v/v ratio) and mobile phase B: 0.1% trifluoroacetic acid in acetonitrile (v/v ratio)) were engaged. The flow rate selected for this study was 1.2 mL min^{-1} . Gradient mode of elution has been used to achieve the required separation, with the following program of isocratic composition between 0 and 15 min with mobile phases A/B of 50/50 v/v, linear gradient composition between 15 and 35 min with mobile phases A/B to 50/50 to 35/65 v/v, isocratic composition between 35 and 55 min with mobile phases A/B to 35/65 v/v, finally equilibrating the run with the initial composition between 56 and 65 min with mobile phases A/B to 50/50 v/v. Thus, the overall run time of this method has been finalized to 65 min. HPLC column was thermostat to a temperature of 32 ± 2 $^\circ\text{C}$. The injection volume for the method was set to 20 μL . The detection and quantification work has been carried out at 258 nm wavelength. The ETV standard, sample and its impurities were found to be adequately soluble with the diluent composition of water/acetonitrile/tetrahydrofuran with a (40/55/5) v/v/v ratio.

Preparation of Stock Solution of ETV Standard And Its Impurities

ETV standard and its impurities were weighed each individually about 7.5 mg and made up to the mark in a 50 mL volumetric flask, dissolved, and diluted to the volume with diluent. These individual solutions (of concentration of each 0.15 mg mL^{-1}) were used as stock solutions for the preparation of further solutions which are used for method validation studies (this is Stock-I).

Preparation of Intermediate Stock Solution of ETV Standard and Its Impurities

An intermediate stock solution of 0.0075 mg mL^{-1} of ETV standard and its impurities were individually prepared by diluting 2.5 mL of the individual Stock solutions-I to separate 50 mL volumetric flasks, and dissolving and diluting to the volume with diluent (this is Stock-II). From this individual stock solution-II, each solution having a concentration of

Table 1 ¹H, and ¹³C NMR chemical shift values (δ ppm) for ETV standard, HMB Impurity, BQN Impurity, Deschloro Impurity and QAM Impurity

Position	ETV		HMB impurity		BQN impurity		Deschloro impurity		QAM impurity	
	¹ H δ (ppm)	¹³ C δ (ppm)	¹ H δ (ppm)	¹³ C δ (ppm)	¹ H δ (ppm)	¹³ C δ (ppm)	¹ H δ (ppm)	¹³ C δ (ppm)	¹ H δ (ppm)	¹³ C δ (ppm)
1	7.35–7.39	126.12	–	176.63	–	176.5	7.14–7.35	131.47	7.16–7.21	131.79
2	7.35–7.39	126.84	–	119.28	–	118.97	7.14–7.35	124.49	7.31–7.37	128.21
3	7.13–7.16	128.36	8.35	127.92	8.22	128.3	7.14–7.35	128.61	7.04–7.10	126.91
4	–	157.63	7.28–7.32	115.2	–	125.75	7.14–7.35	115.27	–	123.78
5	–	120	–	164.05	–	161.86	–	160.57	–	159.21
6	–	139.29	7.55	100.29	7.59	98.65	–	125.85	–	128.57
7	4.19	32.29	–	143.29	–	143.25	3.97–4.06	28.23	4.28	31.59
8	–	127.52	8.9	145.94	8.95	145.88	–	128.3	–	137.93
9	7.87	126.12	–	107.14	–	107.6	7.98	126.2	8.39	131.97
10	–	118.88	–	166.3	–	166.29	–	118.91	–	117.04
11	–	176.18	–	–	–	–	–	176.18	–	173.28
11Ha	–	–	3.75–3.79	60.11	3.77–3.88	60.26	–	–	–	–
11Hb	–	–	3.99	–	3.99	–	–	–	–	–
12	–	107.49	4.85	66.18	4.96	66.47	–	107.18	–	105.38
13	8.88	145.4	2.37–2.38	29.14	2.45	29.2	8.87	145.29	9.26	151.67
14	–	142.41	0.72, 1.15	18.92, 19.10	0.81, 1.20	19.08, 19.19	–	142.33	–	145.61
15	7.49	98.06	–	–	3.99	56.94	7.46	97.99	7.31–7.37	99.17
16	–	161.98	3.99	56.29	–	–	–	161.93	–	169.36
17	–	–	–	–	–	–	–	–	4.21	46.04
17Ha	3.77–3.81	60.19	–	–	–	–	3.77–3.80	60.21	–	–
17Hb	3.98	–	–	–	–	–	3.97–4.06	–	–	–
18	4.9	66.33	–	–	–	–	4.87	66.31	4.45	58.42
19	2.37	29.23	–	–	–	–	2.38	29.24	–	172.82
20, 21	0.73, 1.16	19.00, 19.16	–	–	–	–	0.72, 1.16	18.98, 19.15	–	–
22	–	166.36	–	–	–	–	–	166.42	–	–
23	4.05	56.85	–	–	–	–	3.97–4.06	56.77	–	–
Alcoholic OH	5.22	–	5.18	–	5.25	–	–	–	–	–
Acid OH	15.41	–	15.45	–	15.41	–	15.45	–	–	–

Table 2 ^1H , and ^{13}C NMR chemical shift values (δ ppm) for DFB impurity, 3-Cl-2,4-DFB impurity and leucine impurity

Position	DFB impurity		Methyl ester impurity		3-Cl-2,4-DFB impurity		Leucine impurity	
	^1H δ (ppm)	^{13}C δ (ppm)	^1H δ (ppm)	^{13}C δ (ppm)	^1H δ (ppm)	^{13}C δ (ppm)	^1H δ (ppm)	^{13}C δ (ppm)
1	7.06–7.20	126.40–126.45	7.15–7.28	130.14	7.25–7.37	129.81–130.00	7.16–7.28	130.21
2	7.28–7.37	115.61	7.44–7.50	128.69	7.25–7.37	111.99–112.32	7.46–7.52	128.9
3	7.06–7.20	124.59–124.73	7.15–7.28	125.21	–	154.44–157.77	7.16–7.28	125.33
4	–	146.47–149.89	–	119.58	–	108.11	–	119.62
5	–	148.04–151.47	–	155.64	–	154.98–158.30	–	155.64
6	–	128.66	–	128.52	–	123.62–123.88	–	128
7	4.13	28.02	4.05	28.36	4.1	28.12	4.12	28.46
8	–	127.74	–	125.5	–	126.44	–	127.74
9	8.05	126.45	7.9	127.25	8.06	127.46	8.04	126.51
10	–	118.89	–	121.76	–	118.86	–	118.97
11	–	176.25	–	171.7	–	176.21	–	176.29
12	–	107.37	–	109.54	–	107.35	–	107.36
13	8.88	145.45	8.64	145.71	8.88	145.42	8.83	145.28
14	–	142.44	–	141.62	–	142.43	–	141.88
15	7.47	98.11	7.15–7.28	97.56	7.46	98.15	7.46–7.52	97.74
16	–	161.93	–	160.57	–	161.86	–	161.98
17	–	–	–	–	–	–	3.81	62.21
17Ha	3.82	60.17	3.73–3.80	60.26	3.76–3.80	60.12	–	–
17Hb	3.98–4.04	–	3.91–3.98	–	3.98–4.03	–	–	–
18	4.88	66.33	4.65	65.2	4.87	66.29	5.19–5.22	59.06
19	2.39	29.19	2.31	29.02	2.39	29.14	1.76–1.92	38.94
20, 21	0.73, 1.16	18.94, 19.12	0.74, 1.14	19.07, 19.20	0.73, 1.16	18.92, 19.10	–	–
20	–	–	–	–	–	–	1.44–1.48	24.25
21, 21'	–	–	–	–	–	–	0.87, 0.92	22.32, 22.65
22	–	166.32	–	165.37	–	166.22	–	166.28
23	4.04	56.8	3.73	51.16	4.03	56.78	4.02	56.76
24	–	–	3.98	56.45	–	–	–	–
Alcoholic OH	5.2	–	5.12	–	5.19	–	5.2	–
Acid OH	15.45	–	–	–	15.44	–	15.43	–

0.00045 mg mL⁻¹ was prepared by transferring 3.0 mL of stock solutions to 50 mL volumetric flask, making up the volume with the diluent (This solution is equal to the specification limit of 0.15% w/w).

Preparation of ETV Sample Solution

Weighed about 15 mg of ETV sample was introduced into a 50 mL volumetric flask, dissolved, and diluted to the mark with the diluent. This solution corresponds to the concentration of 0.3 mg mL⁻¹ in the diluent.

Forced Degradation Study Conditions

For thermal and photo-stability stress testing studies, the ETV sample was incubated in an oven at 60 °C for about 48 h for thermal degradation and exposed ETV sample under controlled (opaque) and uncontrolled (photolucent) integrated

light of exposure of visible light of 1.2 million lux hours and UV light of 200 W h m⁻² in a photo-stability chamber for photolytic degradation [28, 29]. To assess the stability indicating the nature of the method, ETV samples were stressed separately by acidic (1N HCl), basic (1N NaOH), and oxidative (5% H₂O₂) stress conditions by adding these stressing agents along with diluent, maintained at elevated temperature condition in a water bath. These final stressed sample solutions were tested to assess whether any degradation occurred.

Preparation of ETV Sample for Acid and Base Degradation Study

Weighed about 15 mg of ETV sample was introduced into a 50 mL volumetric flask, added about 5 mL of diluent to dissolve the sample, then added about 30 mL of 1N hydrochloric acid/1N sodium hydroxide was added and stirred at a constant temperature at 60 °C for about 72 h, then the

Table 3 ^1H , and ^{13}C NMR chemical shift values (δ ppm) for 7-Ethoxy impurity and THP impurity

Position	7-Ethoxy impurity		THP impurity	
	^1H δ (ppm)	^{13}C δ (ppm)	^1H δ (ppm)	^{13}C δ (ppm)
1	7.15–7.29	130.24	6.97–7.07	129.21
2	7.43–7.49	128.69	7.24–7.30	128.84
3	7.15–7.29	125.08	6.97–7.07	124.29
4	–	119.57	–	121.06
5	–	155.64	–	156.42
6	–	128.75	–	127.89
7	4.12	28.77	4.11	28.95
8	–	127.84	–	128.13
9	8.14	126.65	8.27–8.28	128.24
10	–	118.74	–	120.01
11	–	176.29	–	177.11
11Ha	–	–	–	–
11Hb	–	–	–	–
12	–	107.33	–	108.57
13	8.88	145.39	8.91–8.28	144.92
14	–	142.44	–	142.33
15	7.43–7.49	98.59	7.24–7.30	98.81
16	–	161.23	–	162.19
17	–	–	–	–
17Ha	3.75–3.79	60.17	3.73–3.91	62.04
17Hb	3.96–4.04	–	4.15–4.28	–
18	4.85	66.25	4.45–4.55	66.09
19	2.38	29.17	2.44–2.60	29.82
20, 21	0.72, 1.15	18.93, 19.10	–	–
20	–	–	0.83–0.88	19.60, 19.66
21	–	–	1.19–1.25	–
22	–	166.35	–	166.22
23	4.26–4.34	64.79	3.98	55.96
24	1.38	14	4.45–4.55	96.11
25	–	–	1.42–1.78	30.23
26	–	–	1.42–1.78	18.75
27	–	–	1.42–1.78	25.04
28	–	–	3.38–3.56	66.43
Alcoholic OH	5.17	–	–	–
Acid OH	15.49	–	15.19–15.23	–

solution was cooled at room temperature, neutralized with dilute solution of sodium hydroxide for acid degradation and vice versa then, volume made up with diluent, this solution was tested for acid and base degradation study. Blank solution was prepared similarly manner without the addition of ETV sample. When attempted with the higher strengths of base (more than 2N of sodium hydroxide), layer separation was noticed while made up with the diluent; therefore, the degradation studies were restricted with reduced acid and

Table 4 ^1H , and ^{13}C NMR chemical shift values (δ ppm) for dimer impurity

Position	Dimer impurity	
	^1H δ (ppm)	^{13}C δ (ppm)
1	7.12–7.22	130.03
1'	6.73–6.78	128.84
2	7.45–7.49	128.84
2'	7.34–7.39	128.66
3	7.12–7.22	125.18
3'	6.92–6.98	124.88
4	–	119.61
4'	–	119.57
5	–	155.61
5'	–	155.24
6	–	127.99
6'	–	127.62
7	4.11	28.4
7'	3.81–3.89	27.94
8	–	127.73
8'	–	127.14
9, 9'	7.99, 8.02	126.59, 126.96
10, 10'	–	118.77, 119.38
11, 11'	–	176.17, 176.22
12	–	107.43, 108.16
13, 13'	8.89, 9.01	144.37, 145.56
14, 14'	–	142.14, 142.44
15, 15'	7.49, 7.56	97.86, 98.97
16	–	162.04
16'	–	160.17
17	4.83–4.85	68.53
17'Ha	3.81–3.89	60.11
17'Hb	3.94–4.01	–
18	5.41–5.44	63.59
18'	4.83–4.85	66.52
19, 19'	2.42–2.49	28.91, 30.08
20, 20'	0.79	18.87, 19.03
21, 21'	1.18, 1.20	19.11, 19.24
22, 22'	–	166.00, 166.14
23	4.01	56.8
Alcoholic OH	5.22	–
Acid OH', OH''	15.30, 15.33	–

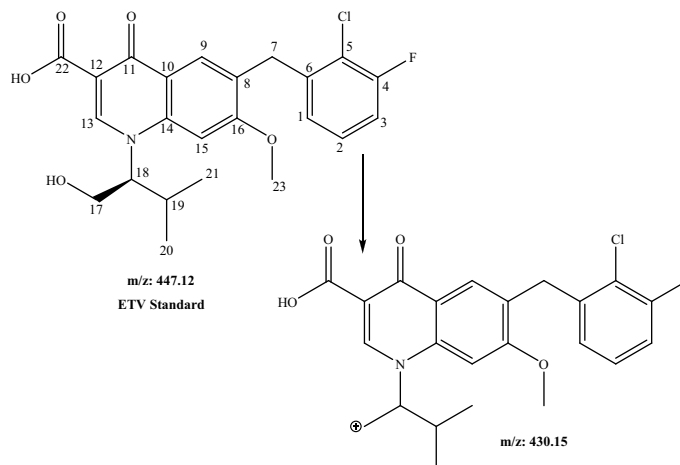
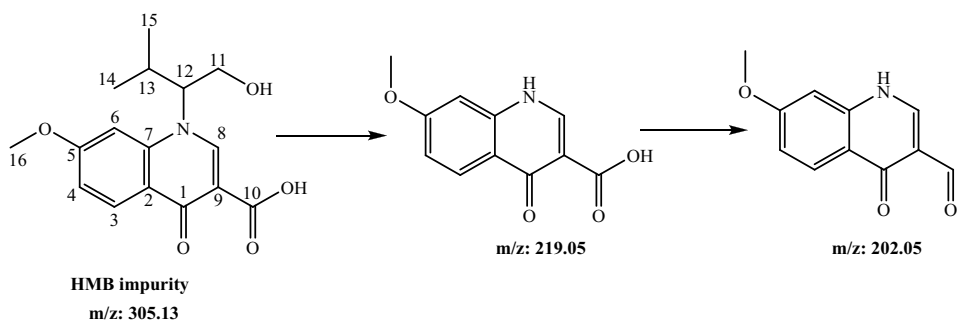
base concentration (i.e., 1N) and the degradation has been facilitated with heat.

Preparation of ETV Sample for Oxidative Degradation Study

Weighed about 15 mg of ETV sample was introduced into a 50 mL volumetric flask, added about 5 mL of diluent to

Table 5 Molecular weight, m/z value, major mass fragments, CAS No, and potency (%w/w) details for each impurity and ETV standard

Name of the impurity	Molecular weight (g mol ⁻¹)	m/z value (M + 1)	Major fragments (m/z)	CAS No	Potency (% w/w)
HMB impurity	305.13	306.3	220.1 & 202.1	–	97.9
BQN impurity	608.24	609.4	548.3, 487.2, 462.2, 431.1 & 315.3	–	96.2
Deschloro impurity	413.45	414.2	396.2, 328.1 & 310.1	2,055,025–82-4	96.8
QAM impurity	375.78	376.0	358.0	–	97.3
DFB impurity	431.15	432.4	414.2, 346.0 & 328.1	–	97.5
methyl ester impurity	461.14	462.2	448.1, 430.6, 378.1, 344.0 & 362.2	1,350,172–03-0	98.2
ETV	447.9	448.3	430.2	697,761–98-1	99.3
3-Cl-2,4- DFB impurity	465.88	466.2	448.2, 434.1, 378.1, 362.1	870,648–11-6	96.9
Leucine impurity	461.14	462.2	-	1,534,364–53-8	98.4
7-Ethoxy impurity	461.14	462.2	444.4 & 358.2	–	97.5
THP impurity	531.18	532.3	514.4 & 430.3	–	99.3
Dimer impurity	863.73	863.2 & 864.1	848.2 & 760.9	–	95.9

Fig. 1 ESI–LC–MS plausible fragments details for ETV standard**Fig. 2** ESI–LC–MS plausible fragments details for HMB impurity

dissolve the sample, then added about 20 mL of 5% hydrogen peroxide and maintained at room temperature for about 72 h, then the solution was volume made up with diluent and tested for oxidative degradation study. A blank solution was also prepared similarly without the addition of ETV sample.

Preparation of ETV Sample for Thermal Degradation Study

About 2 g of ETV sample was spread in a Petri dish, and incubated in an oven at a temperature of 60 °C for about 48 h. Weighed about 15 mg of the above thermal degraded ETV

Fig. 3 ESI–LC–MS plausible fragments details for BQN impurity

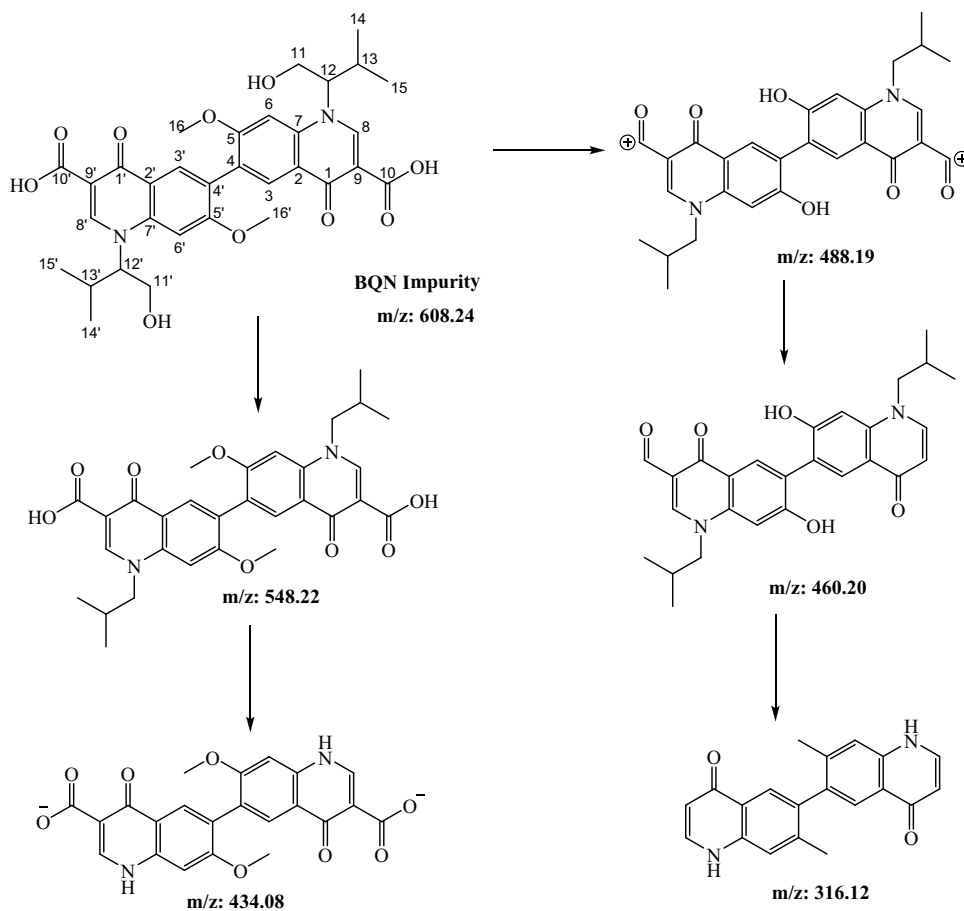


Fig. 4 ESI–LC–MS plausible fragments details for Deschloro impurity

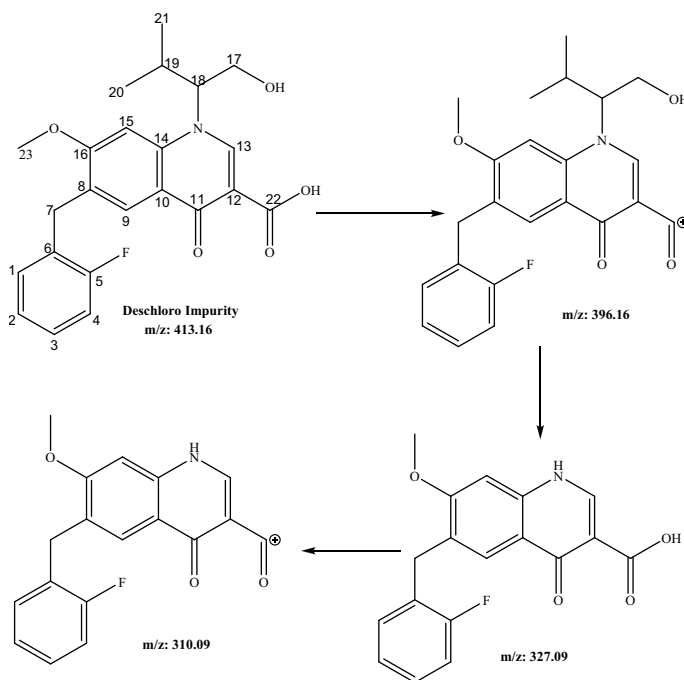


Fig. 5 ESI–LC–MS plausible fragments details for QAM impurity

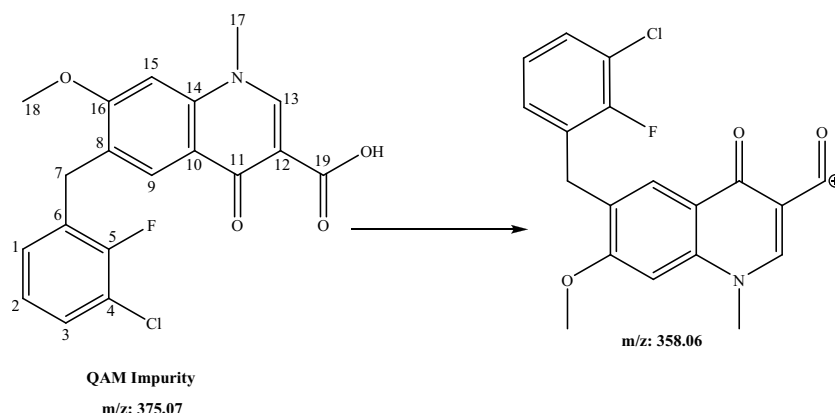
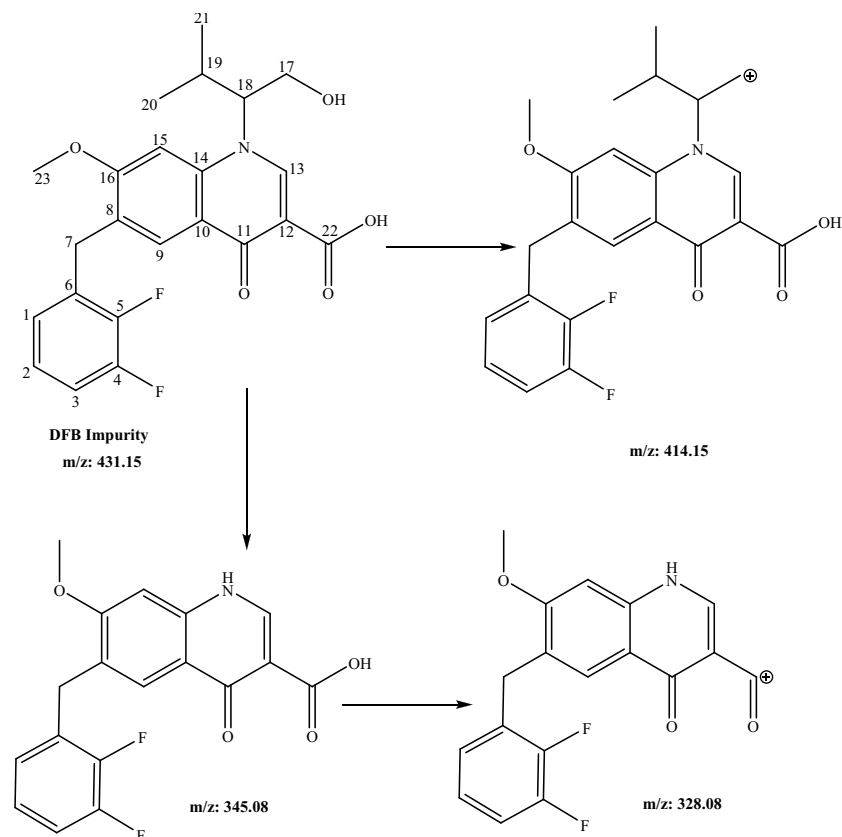


Fig. 6 ESI–LC–MS plausible fragments details for DFB impurity



sample was introduced into a 50 mL volumetric flask, dissolved, and diluted to the mark with the diluent. This sample solution was injected to assess the thermal degradation study.

Preparation of ETV Sample for Photolytic Degradation Study

ETV samples were spread into two separate Petri dishes, one covered with photolucent packing (Uncontrolled), and the other one completely covered with photoopaque packing

(Control). Both of these preparations were exposed in a photostability chamber for the integrated light exposure as specified, once the samples achieved adequate light exposure, both the controlled and the uncontrolled ETV samples were removed from the chamber. From this exposed samples of controlled and uncontrolled, weighed about 15 mg of each ETV samples was introduced into a separate 50 mL volumetric flask, dissolved, and diluted to the mark with the diluent. These sample solutions were injected to assess the photolytic degradation study.

Fig. 7 ESI–LC–MS plausible fragments details for methyl ester impurity

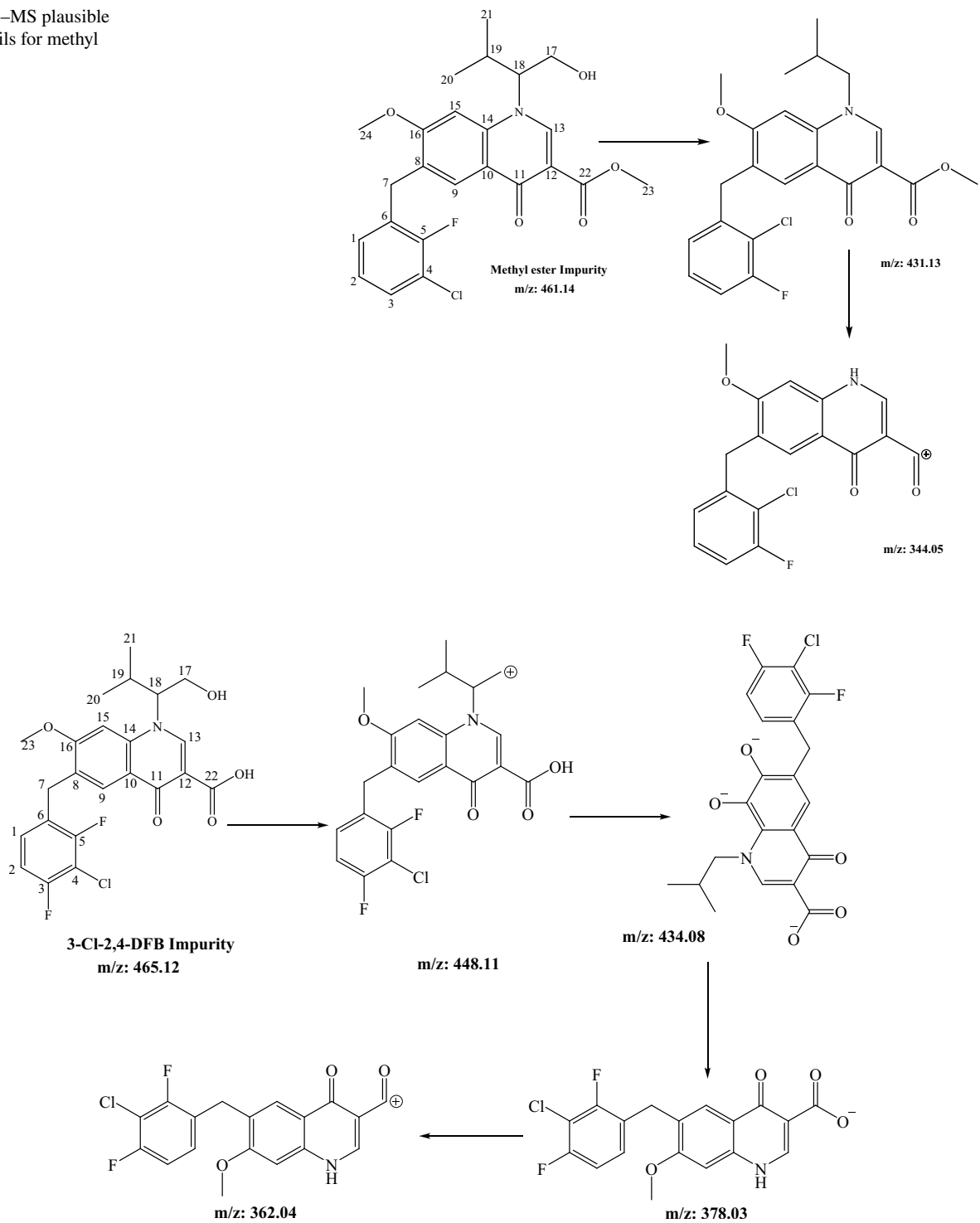


Fig. 8 ESI–LC–MS plausible fragments details for 3-Cl-2,4-DFB impurity

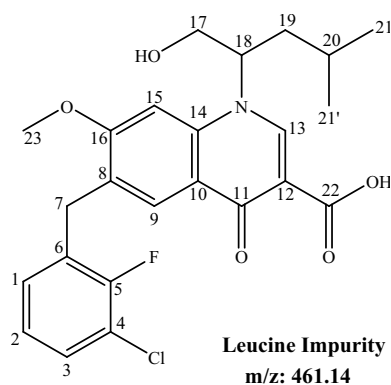
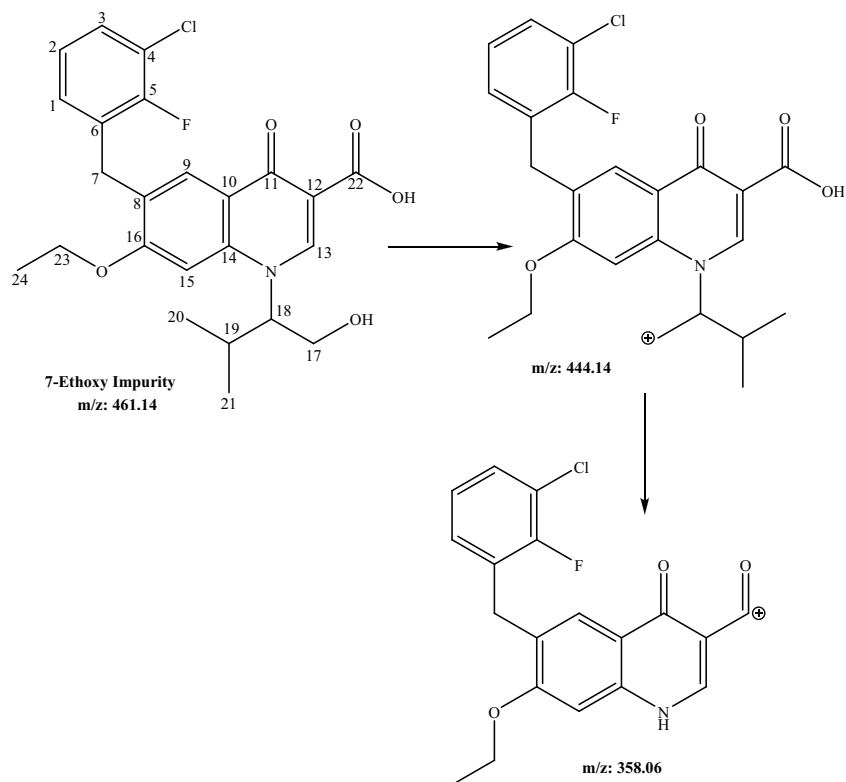


Fig. 9 ESI–LC–MS plausible fragments details for Leucine impurity

Preparation of Solutions for Analytical Method Validation

To evaluate the specificity of the method, the solutions of each impurity were prepared at a concentration of 0.1 mg mL^{-1} in the diluent separately and spiked all of them, each at a concentration of $0.00045 \text{ mg mL}^{-1}$, in the ETV sample. The detection (LOD—Limit of detection), as well as the quantitation (LOQ—Limit of quantitation) limits was established by s/n (the ratio between the signal from the compound and the noise from the baseline) approach to obtain the s/n 3:1 and 10:1 respectively. The final standard solution (which contains ETV standard and all its impurities

Fig. 10 ESI–LC–MS plausible fragments details for 7-Ethoxy impurity



at a concentration of $0.00045 \text{ mg mL}^{-1}$) has been prepared at different levels ranging from 8 to 12% for LOD and 18 to 22% for LOQ. The final LOD and LOQ concentration for each impurity and ETV standard has been arrived based on the acceptance criteria of s/n ratio.

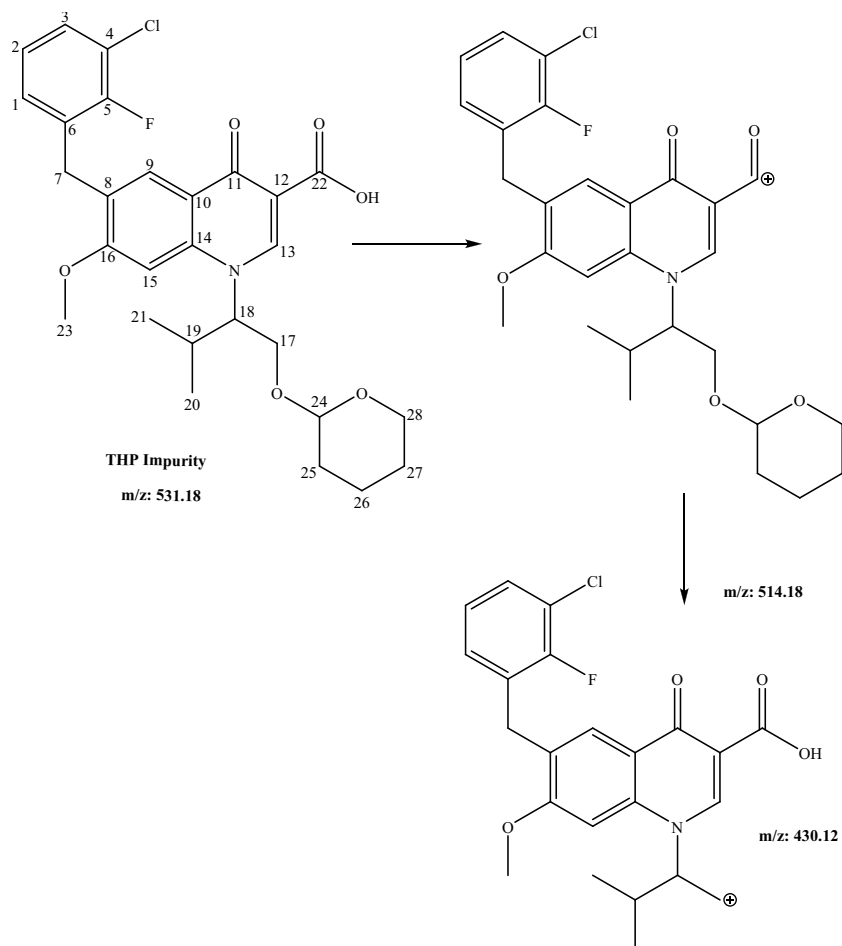
The accuracy study was conducted over four levels i.e., at LOQ, 50 (0.000225), 100 (0.00045), and 120% ($0.00054 \text{ mg mL}^{-1}$), the concentrations of the solutions are with respect to the test concentration of ETV sample (i.e., 0.3 mg mL^{-1}). Linearity has been established with 5 levels ranging from LOQ to 0.00027 , 0.00037 , 0.00045 , and $0.00054 \text{ mg mL}^{-1}$. All these concentrations are with respect to the ETV test concentration. The method precision and the intermediate precision studies were assessed with all impurities spiked in the ETV sample at a concentration of $0.00045 \text{ mg mL}^{-1}$ (which is equal to 0.3 mg mL^{-1} of test concentration).

Results and Discussion

Structural Confirmation Studies Using LC-MS and NMR Techniques

The chemical structures of all the impurities and the ETV standard were elucidated with the aid of ^1H , ^{13}C , and ESI–LC–MS studies [30, 31]. Their fragmentation pattern and purity details have also been reported.

Fig. 11 ESI–LC–MS plausible fragments details for THP impurity



Characterization of ETV standard and Its Impurities

^1H and ^{13}C NMR spectroscopic studies have been performed for ETV standard, and D_2O exchange experiments were also conducted to identify the exchangeable protons. The ^1H -NMR spectrum depicts the chemical shifts ranging from δ 7.13 to 8.88 ppm representing the aromatic protons present at 1–3, 9, 13, and 15th positions. The δ value at 5.22 ppm represents the $-\text{OH}$ proton attached at the 17th position. The chemical shift value at δ 15.41 ppm corresponds to the carboxylic acid proton at the 22nd position. The δ value at 0.73 and 1.16 ppm represents the methyl groups at positions 20 and 21 respectively. The methanolic CH_3 at position 23 exhibited the δ value at 4.05 ppm. The δ value at 4.19 ppm represents the methylene group flanked in between two benzene rings. The diastereotopic protons at 17 exhibited δ values at 3.77–3.81 and 3.98 ppm. The proton of chiral carbon at position 18 exhibited the δ value at 4.90 respectively. The δ value at 2.37 ppm represents the $-\text{CH}$ proton at position 19. From the ^{13}C -NMR spectrum, the δ values at 32.29 and 60.19 ppm represent the methylene carbon atoms at positions 7 and 17 respectively. The δ values at 176.18 and

166.36 ppm represent the carbonyl groups of quinoline-4 (*1H*)-one ring and carboxyl group at positions 11 and 22 respectively. The δ values at 66.33 and 29.23 ppm represent the $-\text{CH}$ carbon atoms at positions 18 and 19 respectively. The δ values at 19.00 and 19.16 ppm represent the $-\text{CH}_3$ carbon atoms at positions 20 and 21 respectively. The δ value at 56.85 ppm represents the methanolic carbon at position 23. Mass spectral analysis was conducted, and the protonated molecular ion was observed at m/z 448 corresponds to $(M + 1)$, the deprotonated molecular ion at m/z value of 446 ($M - 1$), and the m/z value of 506 corresponds to $(M - H + \text{CH}_3\text{COOH})^-$ fragmentation confirms the monoisotopic mass of the molecule as 447. From the mass data, the arrived empirical formula was $\text{C}_{23}\text{H}_{23}\text{ClFNO}_5$.

In the similar way, all other impurities structural elucidation studies have been carried out with the help of ^1H , ^{13}C NMR experiments and their ESI–LC–MS spectral data and also in comparison with ETV standard. The corresponding proton and carbon chemical shift values of NMR data have been tabulated and are available in the Tables 1, 2, 3, and 4. Molecular weight, m/z values, major fragments, CAS No, and their potency value of each impurity and ETV standard

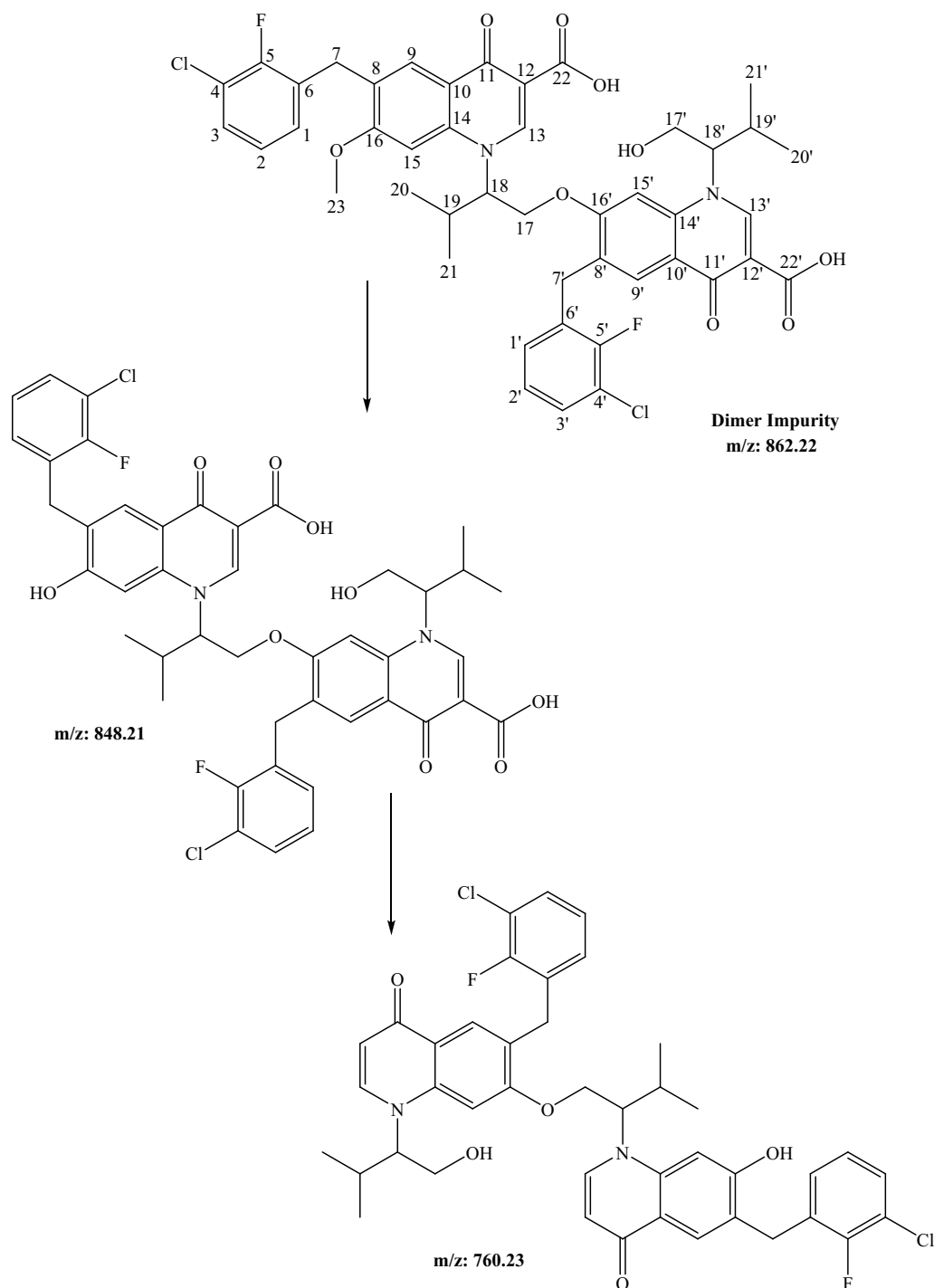


Fig. 12 ESI–LC–MS plausible fragments details for Dimer impurity

are available in Table 5. The major mass fragments to ascertain the structure of ETV standard and each impurity have been deduced and are shown from Figs. 1, 2, 3, 4, 5, 6, 7, 8, 9, 10, 11, and 12. From all these data, chemical name and molecular formula of each impurity have been obtained and are tabulated in the Table 6.

The relevant detailed characterization data and respective spectra of each impurity are included in the supporting information from Table S1 to S12 and Fig. S1 to S36. Respective impurity structures are available from Figs. 1, 2, 3, 4, 5, 6, 7, 8, 9, 10, 11, and 12 of the given chemical name in Table 6.

Table 6 Chemical name and molecular formula for each impurity and ETV standard

Name of the impurity	Chemical name	Molecular formula
HMB impurity	1-(1-hydroxy-3-methylbutan-2-yl)-7-methoxy-4-oxo-1,4-dihydroquinoline-3-carboxylic acid	C ₁₆ H ₁₉ NO ₅
BQN impurity	1,1'-bis(1-hydroxy-3-methylbutan-2-yl)-7,7'-dimethoxy-4,4'-dioxo-1,1',4,4'-tetrahydro-[6,6'-biquinoline]-3,3'-dicarboxylic acid	C ₃₂ H ₃₆ N ₂ O ₁₀
Deschloro impurity	6-(2-fluorobenzyl)-1-(1-hydroxy-3-methylbutan-2-yl)-7-methoxy-4-oxo-1,4-dihydroquinoline-3-carboxylic acid	C ₂₃ H ₂₄ FNO ₅
QAM impurity	6-(3-chloro-2-fluorobenzyl)-7-methoxy-1-methyl-4-oxo-1,4-dihydroquinoline-3-carboxylic acid	C ₁₉ H ₁₅ ClFNO ₄
DFB impurity	6-(2,3-difluorobenzyl)-1-(1-hydroxy-3-methylbutan-2-yl)-7-methoxy-4-oxo-1,4-dihydroquinoline-3-carboxylic acid	C ₂₃ H ₂₃ F ₂ NO ₅
methyl ester impurity	methyl 6-(3-chloro-2-fluorobenzyl)-1-(1-hydroxy-3-methylbutan-2-yl)-7-methoxy-4-oxo-1,4-dihydroquinoline-3-carboxylate	C ₂₄ H ₂₅ ClFNO ₅
ETV	(S)-6-(3-chloro-2-fluorobenzyl)-1-(1-hydroxy-3-methylbutan-2-yl)-7-methoxy-4-oxo-1,4-dihydroquinoline-3-carboxylic acid	C ₂₃ H ₂₃ ClFNO ₅
3-Cl-2,4- DFB impurity	6-(3-chloro-2,4-difluorobenzyl)-1-(1-hydroxy-3-methylbutan-2-yl)-7-methoxy-4-oxo-1,4-dihydroquinoline-3-carboxylic acid	C ₂₃ H ₂₂ ClF ₂ NO ₅
Leucine impurity	6-(3-chloro-2-fluorobenzyl)-1-(1-hydroxy-4-methylpentan-2-yl)-7-methoxy-4-oxo-1,4-dihydroquinoline-3-carboxylic acid	C ₂₄ H ₂₅ ClFNO ₅
7-Ethoxy impurity	6-(3-chloro-2-fluorobenzyl)-7-ethoxy-1-(1-hydroxy-3-methylbutan-2-yl)-4-oxo-1,4-dihydroquinoline-3-carboxylic acid	C ₂₄ H ₂₅ ClFNO ₅
THP impurity	6-(3-chloro-2-fluorobenzyl)-7-methoxy-1-(3-methyl-1-((tetrahydro-2H-pyran-2-yl)oxy)butan-2-yl)-4-oxo-1,4-dihydroquinoline-3-carboxylic acid	C ₂₈ H ₃₁ ClFNO ₆
Dimer impurity	1-(1-((3-carboxy-6-(3-chloro-2-fluorobenzyl)-1-(1-hydroxy-3-methylbutan-2-yl)-4-oxo-1,4-dihydroquinolin-7-yl)oxy)-3-methylbutan-2-yl)-6-(3-chloro-2-fluorobenzyl)-7-methoxy-4-oxo-1,4-dihydroquinoline-3-carboxylic acid	C ₄₅ H ₄₂ Cl ₂ F ₂ N ₂ O ₉

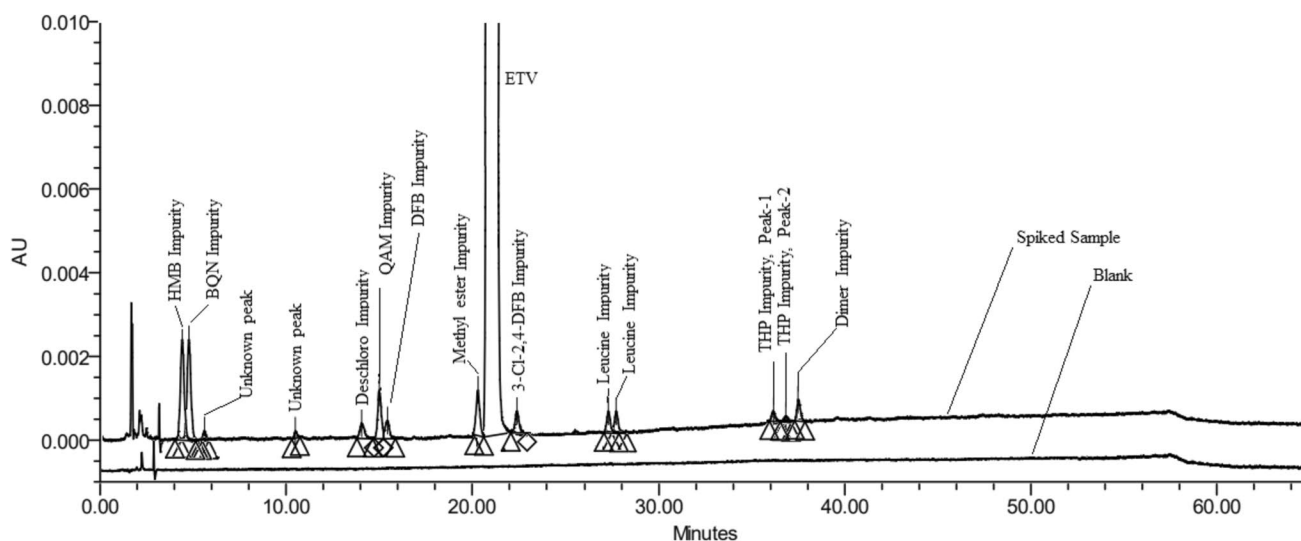


Fig. 13 Alltima C18 (250 mm length × 4.6 mm width, 3 μm as particle size), (MP)—A (0.1% orthophosphoric acid solution) and (MP)—B (100% acetonitrile), isocratic elution mode with MP-A/B 70/30 v/v for 60 min as run time. Column temperature 30 °C; Flow

rate: 1.2 mL min⁻¹. Injection volume 20 μL, UV detection at 258 nm. Sample concentration: 0.3 mg mL⁻¹ in water:acetonitrile:tetrahydrofuran (40/55/5, v/v/v)

The pharmacologically active isomer of ETV is (S)-Isomer. The isomerism of other impurities has not been studied and not reported anywhere in the literature. Thus, normal notation has been used.

HPLC Method Development

The ETV standard and its related impurities were synthesized in-house, and were characterized, their structures were confirmed. Potency of each impurity has been calculated.

Table 7 Resolution between two closely eluting peaks, tailing factor, theoretical plates, % RSD for 6 replicate injections of ETV standard

Column details	Resolution between two closely eluting pairs					
	HMB & BQN impurity	Deschloro & QAM impurity	QAM & DBF impurity	Methyl ester impurity & ETV	ETV & 3-Cl,2-4-DFB impurity	Leucine & 7-Ethoxy impurity
Aqua C18	2.4	1.3	2.5	3.0	1.9	1.5
Alltima C18	2.0	1.3	2.3	2.8	2.3	1.6
Unison UK C18	2.5	1.5	1.9	2.1	4.2	1.6
Peerless basic C18	2.8	1.8	2.7	3.2	5.5	1.8
Column details	For ETV peak			Theoretical plate	% RSD for 6 replicate injections	
	Tailing factor					
Aqua C18	1.2		37,790	3.2		
Alltima C18	1.1		40,098	2.1		
Unison UK C18	0.98		41,076	1.9		
Peerless basic C18	1.01		46,583	0.8		

Table 8 Retention time (RT), relative retention time (RRT), purity angle, and purity threshold of each impurity are shown as part of the specificity study

Name of the impurity	Retention Time (min)	RRT	Purity angle	Purity threshold
HMB impurity	4.26	0.21	1.25	1.91
BQN impurity	4.61	0.22	1.05	1.93
Deschloro impurity	13.84	0.67	2.02	3.10
QAM impurity	14.28	0.69	1.40	3.09
DBF impurity	15.19	0.73	1.30	2.73
methyl ester impurity	19.42	0.94	2.01	3.65
ETV	20.74	1.00	0.05	1.01
3-Cl-2,4- DFB impurity	22.86	1.10	1.83	3.72
Leucine impurity	26.94	1.30	1.83	3.70
7-Ethoxy impurity	27.47	1.32	1.72	3.12
THP impurity peak-1	39.83	1.92	3.11	5.84
THP impurity peak-2	40.32	1.94	4.00	6.20
Dimer impurity	47.51	2.29	2.76	4.94

The primary aim of the analytical method development has been set to separate all these eleven impurities from the main drug (ETV) using a stability indicating related substances by HPLC method [32, 33]. ETV is Ames-negative, thus non-genotoxic in nature. All the impurities of ETV are also confirmed as non-genotoxic in nature. Therefore, these impurities are ordinary impurities and thus the specification limit for each impurity has been set as 0.15%.

In order to choose the appropriate wavelength for this HPLC study, all the impurities and ETV standard have been prepared individually at a concentration of 10 ppm each (water and acetonitrile was used as diluent with 60:40 v/v ratio), each solution was scanned for their UV absorption at 200–400 nm range. All the impurities and ETV standard exhibited maximum absorption around 258 nm, and thus

the detection wavelength for the method has been chosen at 258 nm.

The diluent selection study has been carried out by studying their solubility. All the impurities and ETV standard were found adequately soluble in the mixture of water and acetonitrile. Clear solutions were obtained when test tube trial was conducted. Water and acetonitrile were used as initial diluent. With this composition, the peak shapes were slightly distorted, noticed with tailing, therefore to improve the peak shape and make them symmetry. About 5% of tetrahydrofuran was added in the diluent. Thus, the final diluent was fixed to water/acetonitrile/tetrahydrofuran of 40/55/5 v/v/v ratio, which had improved the peak shape, the area reproducibility, and the theoretical plate. The standard, the sample, and the spiked sample solutions were also found to

be stable, which indicates that the diluent chosen was compatible for this study.

The dissociation constant (pKa) for ETV was found 6.6 [34]. Thus, the initial scouting studies were conducted at acidic pH, i.e., mobile phase (MP)—A (0.1% orthophosphoric acid solution) and mobile phase (MP)-B (100% acetonitrile), using isocratic elution mode with two different compositions i.e., (1) MP-A/B 70/30 v/v and (2) MP-A/B 30/70 v/v, and (3) with linear gradient composition of MP-A/B as 70/30 at initial time and 30/70 v/v at 60 min. The separation was carried out using with Alltima C18 HPLC Column. In the first trial, the impurities methyl ester, 3-Cl-2,4-DFB impurity, ETV, THP impurity, and Dimer impurity peaks could not be separated well (Fig. 13). Whereas in the second trial, the peaks were clustered without effective separation. At the third trial of linear gradient elution, separations of all the peaks were achieved; however, poor resolution was noticed between the peaks of (1) HMB impurity and BQN impurity (2) Deschloro impurity, QAM impurity, and DFB impurity (3) Leucine impurity and 7-Ethoxy impurity were also merged.

From all the initial scouting studies using different mobile phase compositions, it was understood that linear gradient throughout the run might not be beneficial to separate all the impurities. Therefore, time-based gradient program must be customized based on the elution. Two initial isocratic compositions of mobile phase A/B with 60/40 and 50/50 v/v were tested, in which the composition of 50/50 was found optimum for the first portion of the elution program. The linear composition was optimized with the mobile phase compositions of A/B to 50/50 and 35/65 v/v for the second portion of the gradient program where majority of the impurities elute. Then subsequently this increased organic ratio to elute, the non-polar impurities, followed by equilibrating the column to make it ready for the next run, which has been designed within the selected run time of the gradient program. Thus, further trials were conducted using 0.05, 0.1% trifluoroacetic acid, formic acid, and 5–20 mM potassium dihydrogen phosphate buffer of pH 4, which were evaluated as aqueous phase compositions for mobile phase A. Better separation was achieved when phosphoric acid as well as trifluoroacetic acid aqueous mobile phases was tested individually. When tested with both the mobile phase A compositions (i.e., 0.1% v/v phosphoric acid and trifluoroacetic acid) individually, the obtained impurity profiles are similar. However, in order to carry out mass spectrometric analysis for impurities characterization and to implement mass compatible mobile phase, trifluoroacetic acid was chosen as the aqueous phase for our HPLC analysis. Different brands of analytical columns which include Alltima C18, Aqua C18, Unison UK C18, and Peerless Basic C18 (Fig. 14) were tested to check for better separation and peak shape. In

all the columns tested, better separation, peak shape, and considerable theoretical plate for each peak, % RSD for 6 replicate injections of dilute ETV standard solution were observed only with Peerless Basic C18 column (Table 7).

The main peak (ETV) was eluted at a retention time of about 21 min, and all the impurities were separated within 50 min and the entire run time has been finalized to 65 min. The THP impurity exhibits two peaks which are due to the (SS) and (SR) diastereomers as this impurity possesses two chiral centers, i.e., one carbon which is connected to the nitrogen atom and the other carbon which is connecting the tetrahydropyran. Thus, for quantification purpose, both the peaks were added up together and the sum of area was used for all quantification works.

Analytical Method Validation

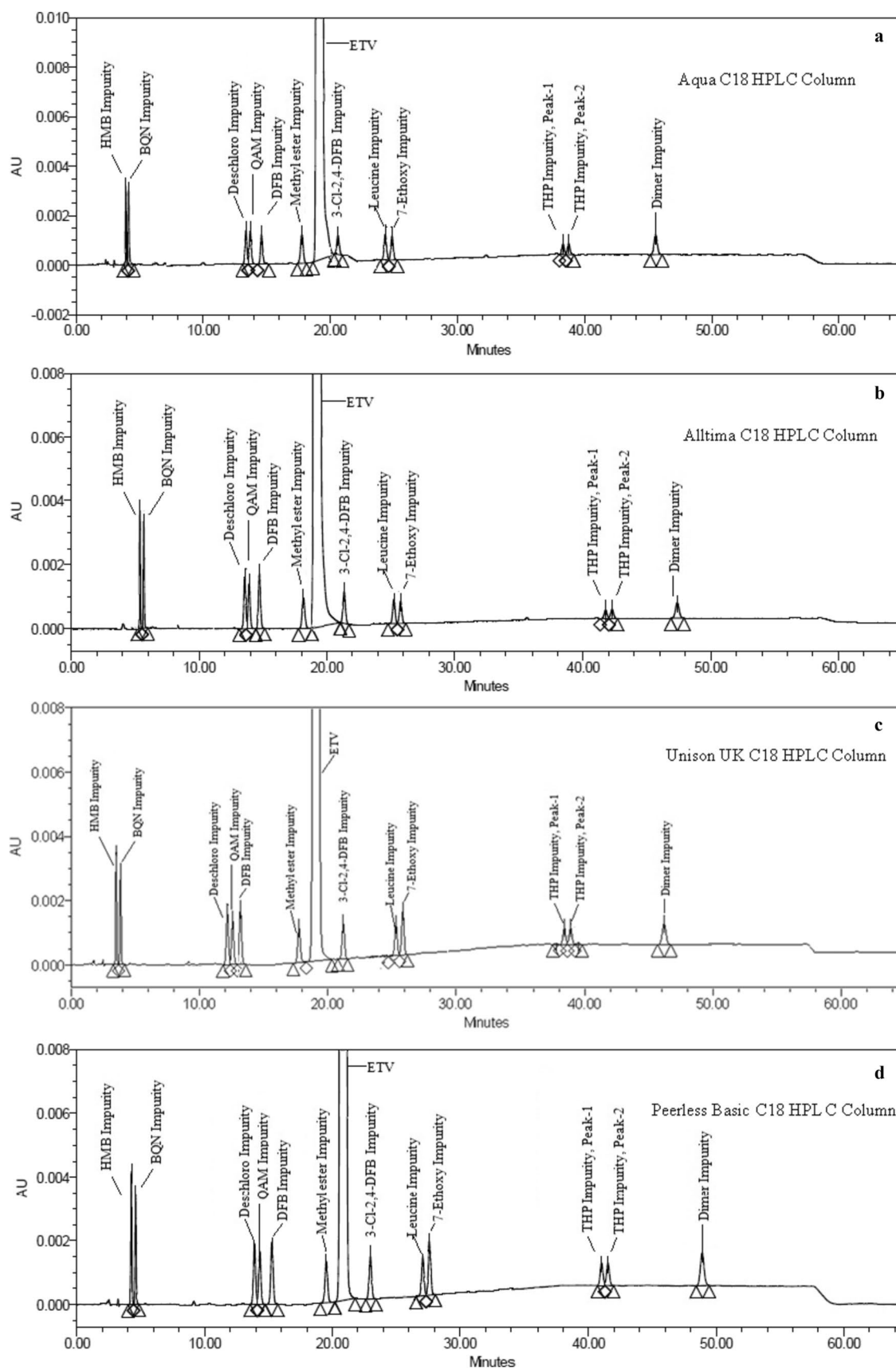
To evaluate the method's capability, and to yield consistent results over time and across laboratories, the developed analytical-related substances method was inflicted to the validation process according to the ICH Q2 R1 guideline [35]. The following were the predefined method parameters which include system suitability, system precision, specificity, forced degradation, the limit of detection (LOD) and limit of quantitation (LOQ), linearity, accuracy, method and intermediate precision, robustness, mobile phase, and solution stability studies, the method was fully validated for the intended application [36, 37].

Forced Degradation

In all the stressed conditions of acidic, basic, oxidative, thermal, and photodegradation studies, the ETV sample was found to be stable. There was no degradation reported in any of the degradation conditions even at a 1% level against the requirement of 5–30% to account for primary degradation. Therefore, the compound is considered as a thermally stable compound.

Specificity

Specificity is the ability to assess unequivocally the analyte in the presence of other components which may be expected to be present or interfere with the peaks of interest. Typically, they could be impurities, degradants, and matrix components. All the process-related impurities and ETV peaks were well separated from each other (resolution not <1.2), and no co-elution or interference was observed between any two closely eluting peaks, which was further confirmed by the homogeneity study through peak purity testing (reported the purity angle and threshold values) in which the peaks are considered pure when purity angle is less than that of the purity threshold value (Table 8) [38, 39]. The peak purity



◀**Fig. 14** Chromatogram on different columns **a** Aqua C18, **b** Alltima C18, **c** Unison UK C18 & **d** Peerless Basic C18, (250 mm length × 4.6 mm width, 3 μm as particle size), Mobile phase A: 0.1% trifluoroacetic acid in water and Mobile phase B 0.1% trifluoroacetic acid in acetonitrile, Gradient program: 0–15 min A/B of 50/50 v/v, 15–35 min A/B to 50/50–35/65 v/v, 35–55 min /B to 35/65 v/v, 56–65 min A/B to 50/50 v/v. Column temperature 30 °C; Flow rate: 1.2 mL min⁻¹. Injection volume 20 μL, UV detection at 258 nm

spectra of ETV and its impurities were recorded using a PDA detector (Fig. 15).

Accuracy

The accuracy (an agreement study between the theoretical amount to the recovered amount) was performed by spiking all the process-related impurities in an ETV sample of 0.3 mg mL⁻¹ concentration at four levels starting from LOQ, 0.075% (0.000225 mg mL⁻¹ = 50% of target concentration), 0.15% (0.00045 mg mL⁻¹ = 100% of target concentration) and 0.18% (0.00054 mg mL⁻¹ = 120% of target concentration). The percentage recovery was calculated between the recovered amount after analysis and the theoretical amount of analyte added to the sample to study recovery and is available in Table 9.

LOD, LOQ, Linearity, and Range

LOD and LOQ for each impurity have been obtained using the conventional *s/n* ratio approach. For LOD, the targeted concentrations were to possess the *s/n* to 3:1. Whereas for the LOQ level, the targeted concentrations were to possess the *s/n* to 10:1. The determined LOD concentrations were about 15% of the actual specification limit and the LOQ concentrations were about 30% to the target concentration of the ETV sample. The obtained lower levels of detection as well quantification levels enhance the method detection capability.

The linearity was established over five different concentration levels of the ETV standard and all the impurities (absolute concentration is 0.00045 mg mL⁻¹, the target level i.e., 100%) starting from LOQ solutions, 60% solution (0.00027 mg mL⁻¹), 80% solution (0.00037 μg mL⁻¹), 100% solution (0.00045 mg mL⁻¹), and 120% solution (0.00054 mg mL⁻¹). Each concentration was injected in triplicate to assess the concordance of injection and the average area was used to infer linearity by plotting the area on the y-axis and the concentration on the x-axis. The regression coefficient (*r*²) for each impurity was >0.999 for (*n* = 5). The linearity range, slope and intercept equation, y-intercept bias, and relative response factor (RRF-dividing the slope value of impurity against the slope value of ETV standard) were calculated and reported in Table 10.

Method Precision & Intermediate Precision (Intraday and Inter-day precision)

The method precision (Intraday) and Intermediate precision (Inter-day) studies were performed by spiking all the impurities at the target level concentration (0.15% = 0.00045 mg mL⁻¹ absolute concentration) in the ETV sample. Six different ETV samples (at concentration of 0.3 mg mL⁻¹) spiked with all the impurities at 0.00045 mg mL⁻¹ concentration levels were prepared and analyzed on different days, with two different analysts, with different instruments, columns, and reagents. The recovery of each impurity in the spiked ETV samples was calculated. The method precision (MP) and intermediate precision (IP) results were computed, and the obtained standard deviation (SD) and % RSD for each impurity were less than 5, indicating that there is a good agreement between MP and IP studies. The obtained results are tabulated in Table 11.

Mobile Phase and Solution Stability

The mobile phase and solution stability studies were conducted by spiking all the impurities at the target level concentration (0.45 μg mL⁻¹) into the ETV sample (0.3 mg mL⁻¹ concentration). The solutions of all impurities standard, ETV sample, and all impurities spiked into the ETV sample were individually transferred into two different volumetric flasks equally. One part was stored at room temperature and the other part was preserved at 2–8 °C in the laboratory refrigerator. Before transferring, the initial analysis was conducted using freshly prepared solutions, each solution was injected after the 48 h interval, and the system suitability and recovery for each impurity were compared against the initial and after 48 h. Further, system suitability solutions were prepared freshly for initial and after 48 h, and tested for the system suitability criteria using the same mobile phase. The satisfactory results indicate that the solutions are stable and could be used by storing over 48 h in room temperature. However, for better stability over the specified time point, they could be stored at 2–8 °C. The mobile phase was found to be stable without any physical change (clear without any turbidity or cloudiness) and therefore mobile phase is stable up to 48 h. The standard, sample, and the spiked sample solution were placed at room temperature as well as at 2–8 °C were also stable up to 48 h, the obtained results are tabulated in Table 12.

Application of Method

Three different manufacturers ((1) Zhejiang Ausan Pharmaceuticals, China. (2) Shanghai Desano Chem, China and (3) JL Pharm, China) commercial lot samples were obtained. They were tested for the fate of the reported impurities in

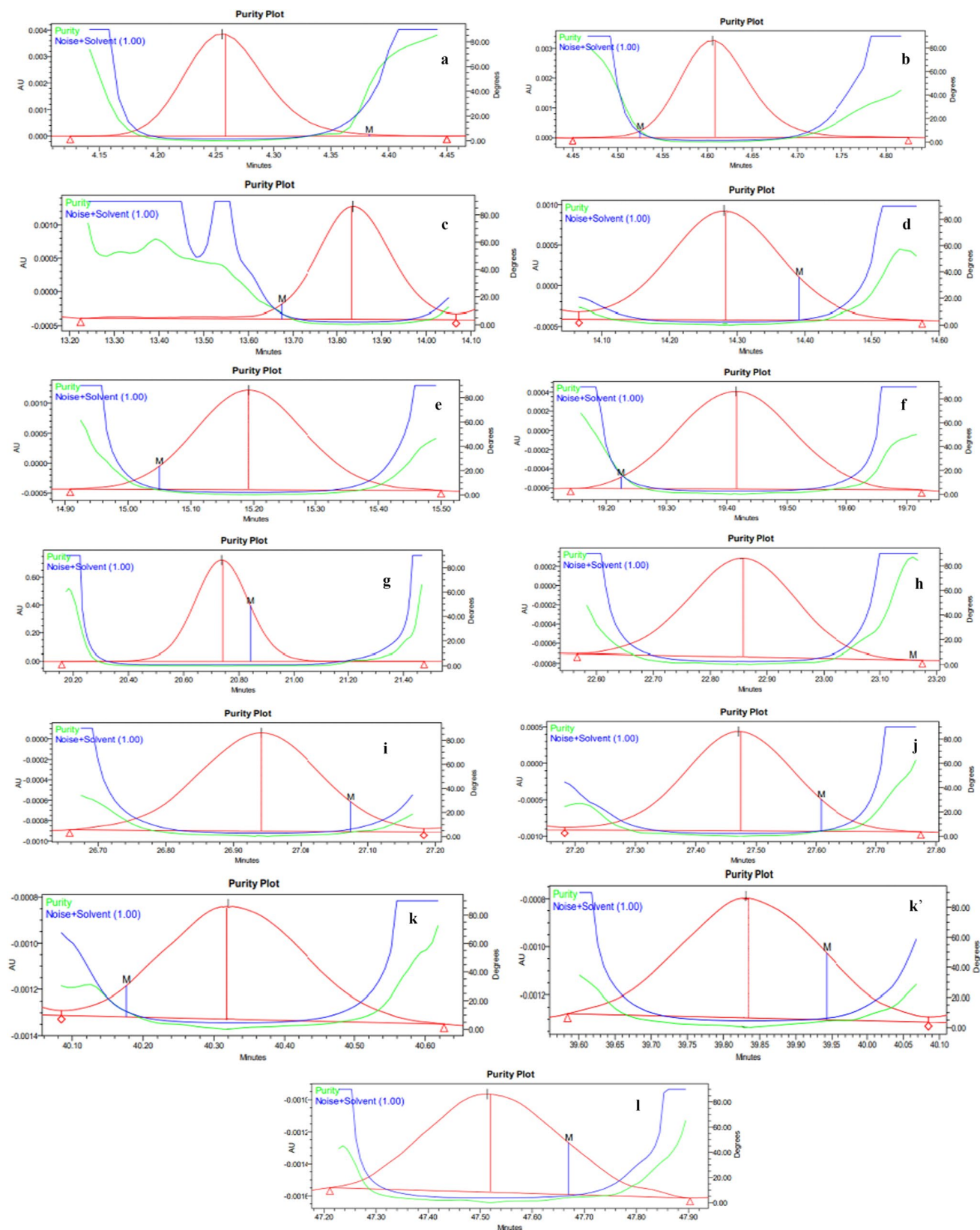


Fig. 15 Peak purity plot for ETV standard and its each impurity generated on PDA detector of HPLC system

Table 9 % recovery results for all the impurities spiked in the ETV sample at four levels i.e., LOQ, 50, 100, and 120% to the target ETV sample concentration as part of the accuracy study

Name of the impurity	Accuracy (% mean recovery ^a ± SD)			
	At LOQ level	At 50% level	At 100% level	At 120% level
HMB impurity	104.3 ± 2.5	104.7 ± 1.4	100.4 ± 0.9	99.2 ± 1.2
BQN impurity	99.4 ± 1.7	100 ± 1.6	99.3 ± 2.0	98.3 ± 1.2
Deschloro impurity	99.5 ± 1.0	97.7 ± 3.0	104.2 ± 1.3	103.0 ± 1.5
QAM impurity	100.2 ± 1.9	98.9 ± 1.5	102.6 ± 1.3	100.3 ± 0.2
DFB impurity	97.9 ± 0.8	98.6 ± 0.8	100.5 ± 1.4	100.0 ± 0.7
methyl ester impurity	101.4 ± 3.0	99.7 ± 1.5	101.0 ± 2.0	100.2 ± 0.6
3-Cl-2,4- DFB impurity	103.1 ± 1.8	103.0 ± 3.9	100.0 ± 1.1	98.5 ± 1.0
Leucine impurity	102.3 ± 1.1	100.5 ± 0.4	100.4 ± 0.4	100.3 ± 0.3
7-Ethoxy impurity	102.5 ± 0.6	103.2 ± 0.7	103.7 ± 0.3	103.3 ± 0.2
THP impurity	101.6 ± 1.7	102.5 ± 0.7	98.1 ± 0.3	98.3 ± 0.5
Dimer impurity	100.9 ± 2.2	99.1 ± 2.4	98.1 ± 0.5	98.4 ± 1.2

^a*n* = 3 different preparations were made and the average results are calculated**Table 10** LOD, LOQ and Linearity range, regression coefficient (*r*²), slope and intercept equation, y-intercept bias, and relative response factor (RRF) for each impurity and ETV standard

Impurity	LOD (% w/w)	LOQ (% w/w)	Linearity range (%w/w)	<i>r</i> ²	Slope and intercept Equation	Y-intercept bias	RRF
HMB impurity	0.016	0.031	0.031–0.122	0.9996	$y = 44611937x - 151.4$	-0.74	1.98
BQN impurity	0.016	0.031	0.031–0.122	0.9996	$y = 39464178x - 231.6$	-1.30	1.75
Deschloro impurity	0.016	0.029	0.029–0.120	0.9999	$y = 37372917x + 153.8$	0.91	1.66
QAM impurity	0.013	0.031	0.031–0.120	0.9998	$y = 38195863x + 186.2$	1.07	1.70
DFB impurity	0.016	0.031	0.031–0.120	0.9992	$y = 36452364x - 93.8$	-0.57	1.62
methyl ester impurity	0.018	0.031	0.031–0.124	0.9990	$y = 33449903x + 154.4$	0.98	1.49
ETV	0.016	0.031	0.031–0.122	0.9996	$y = 22596210x - 18.9$	-0.18	1.00
3-Cl-2,4- DFB impurity	0.016	0.029	0.029–0.118	0.9991	$y = 34694150x + 36.9$	0.24	1.54
Leucine impurity	0.016	0.029	0.029–0.120	0.9992	$y = 31253668x + 31.0$	-0.22	1.40
7-Ethoxy impurity	0.016	0.029	0.029–0.120	0.9998	$y = 37402311x - 99.2$	-0.59	1.66
HP impurity	0.016	0.031	0.031–0.124	0.9979	$y = 28716965x + 136.8$	1.03	1.28
Dimer impurity	0.016	0.031	0.031–0.120	0.9992	$y = 29223917x - 14.3$	-0.11	1.30

Table 11 Results for Method precision and intermediate precision studies

Name of the impurity	Theoretical concentration (% w/w)	Method precision concentration (% w/w) (Mean ± SD)	Measured RSD%	Intermediate precision concentration (%w/w) (Mean ± SD)	Measured RSD%
HMB impurity	0.15	0.15 ± 0.000	0.0	0.15 ± 0.000	0.0
BQN impurity	0.15	0.14 ± 0.005	3.6	0.15 ± 0.004	2.8
Deschloro impurity	0.15	0.15 ± 0.005	3.4	0.15 ± 0.005	3.5
QAM impurity	0.15	0.15 ± 0.004	2.7	0.15 ± 0.000	0.0
DFB impurity	0.15	0.15 ± 0.000	0.0	0.15 ± 0.000	0.0
methyl ester impurity	0.15	0.15 ± 0.000	0.0	0.15 ± 0.000	0.0
ETV	0.15	0.15 ± 0.000	0.0	0.15 ± 0.004	2.7
3-Cl-2,4- DFB impurity	0.15	0.15 ± 0.000	0.0	0.15 ± 0.000	0.0
Leucine impurity	0.15	0.15 ± 0.004	2.7	0.15 ± 0.000	0.0
7-Ethoxy impurity	0.15	0.14 ± 0.004	2.9	0.15 ± 0.005	3.8
THP impurity	0.15	0.15 ± 0.000	0.0	0.15 ± 0.005	3.5

Table 12 Solution stability and mobile phase stability studies results

Name of the impurity	Initial (% w/w)	After 48 h (% w/w) at RT ^a	% relative to initial	After 48 h (% w/w) at 2–8 °C	% relative to initial
HMB impurity	0.15	0.15	–	0.15	–
BQN impurity	0.15	0.14	6.7	0.15	–
Deschloro impurity	0.15	0.15	–	0.15	–
QAM impurity	0.15	0.15	–	0.15	–
DFB impurity	0.15	0.15	–	0.15	–
methyl ester impurity	0.15	0.15	–	0.15	–
ETV	0.1	0.1	–	0.1	–
3-Cl-2,4- DFB impurity	0.15	0.15	–	0.15	–
Leucine impurity	0.15	0.15	–	0.15	–
7-Ethoxy impurity	0.15	0.15	–	0.15	–
THP impurity	0.15	0.15	–	0.15	–
Dimer impurity	0.15	0.15	–	0.15	–

^aSpiked samples when stored at ambient temperature (between 15 and 30 °C)

Table 13 Commercial lot sample analysis results from different manufacturers

Name of the impurity ^a	Manufacturer-1	Manufacturer-2	Manufacturer-3
HMB impurity	Not detected	BDL (0.09%)	BDL (0.015%)
BQN impurity	Not detected	BDL (0.013%)	Not detected
Deschloro impurity	Not detected	BDL (0.07%)	BQL (0.025%)
QAM impurity	Not detected	Not detected	Not detected
DFB impurity	BQL (0.022%)	Not detected	Not detected
methyl ester impurity	Not detected	Not detected	Not detected
ETV	99.42	99.55	99.61
3-Cl-2,4- DFB impurity	Not detected	Not detected	Not detected
Leucine impurity	Not detected	Not detected	Not detected
7-Ethoxy impurity	BDL (0.011%)	BQL (0.021%)	BQL (0.017%)
THP impurity	BDL (0.012%)	Not detected	Not detected
Dimer impurity	BDL (0.010%)	BDL (0.019%)	BDL (0.017%)

^aAll these samples contain the reported impurities almost below quantification level

this research work. The obtained results are tabulated under the Table 13.

Conclusion

ETV is a modern INSTs drug which is used alone or in combination with other drugs for the effective treatment of antiretroviral therapy. As the drug belongs to a modern class of therapy, there is not much information available about the impurity profile of this drug, their degradation pathway, and the analytical methods engaged for the quantitative estimation of its impurities. In this research work, we have identified eleven process-related impurities which have not been reported anywhere before in the literature. We have carried out structural identification study for all the impurities with the help of ¹H, ¹³C, and ESI–LC–MS spectroscopy

techniques, confirmed their structures with the help of NMR data, proposed the plausible fragments for each impurities with the help of mass spectral data. Simple and mass spectrometry compatible HPLC method has been developed for the separation of all the eleven process-related impurities from its drug substance. The degradation study has been conducted to assess the degradation behavior of the drug substance. The method has been fully validated with specificity, LOD, LOQ, precision, accuracy, linearity, and solution stability, which has also been established. In order to extend the method adoptability, three different manufacturer samples were also obtained, tested, and reported—the levels of each impurity quantified in this method for comparison and to impart the quality of the drug substances available in the market. Thus, this method shall also be engaged as quality inferring tool for the marketed samples.

Supplementary Information The online version contains supplementary material available at <https://doi.org/10.1007/s10337-024-04314-2>.

Author contributions Elumalai performed the experimental work, Sellappan, Mamidala, Nishtala, and Thenmozhi wrote the main manuscript. All authors reviewed the manuscript.

Data availability The datasets generated and analyzed during the current study are available from the corresponding on reasonable request.

Declarations

Conflict of interests The authors declare no competing interests.

References

- Prada N, Markowitz M (2010) Novel integrase inhibitors for HIV. *Expert Opin Investig Drugs* 19:1087–1098. <https://doi.org/10.1517/13543784.2010.501078>
- Siberry GK, Hazra R (2018) 113-Management of HIV infection. In: Long SS, Fischer M, Prober CG (eds) principles and practice of pediatric infectious diseases, 5 edn. Elsevier, Amsterdam, p 681.e2. <https://doi.org/10.1016/B978-0-323-40181-4.00113-4>
- Eckhardt BJ, Gulick RM (2017) 152—drugs for HIV infection. In: Cohen J, Powderly WG, Opal SM (eds) Infectious diseases, 4 edn. Elsevier, Amsterdam, pp 1293–1308. e2. <https://doi.org/10.1016/B978-0-7020-6285-8.00152-0>
- Tsibris AMN, Hirsch MS (2015) 130—antiretroviral therapy for human immunodeficiency virus infection. In: Bennett JE, Dolin R, Blaser MJ, Mandell, Douglas (eds) Principles and practice of infectious diseases, 8 edn. WB Saunders, Elsevier, Amsterdam, pp 1622–1641. e6. <https://doi.org/10.1016/B978-1-4557-4801-3.00130-2>
- Waller DG, Sampson AP (2018) 51—chemotherapy of infections. In: Waller DG, Sampson AP (eds) Medical pharmacology and therapeutics, 5 edn. Elsevier, Amsterdam, p 581. <https://doi.org/10.1016/B978-0-7020-7167-6.00051-8>
- Brody T (2018) Chapter 4—dose modification and dose titration. In: Brody T (ed) FDA's Drug review process and the package label. Academic Press, Cambridge, p 101. <https://doi.org/10.1016/B978-0-12-814647-7.00004-X>
- Isobel DR, Jodi ML, Catherine PO, Ana LGC, Li HK, Barker CIS (2014) Chapter 29—antiviral drugs. In: Ray SD (ed) Side effects of drugs annual. Elsevier, Amsterdam, pp 36: 401. <https://doi.org/10.1016/B978-0-444-63407-8.00029-0>
- Brehm TT, Franz M, Hüfner A, Hertling S, Schmiedel S, Degen O, Kreuels B, Wiesch JSZ (2019) Safety and efficacy of elvitegravir, dolutegravir, and raltegravir in a real-world cohort of treatment-naïve and -experienced patients. *Medicine (Baltimore)* 98:e16721. <https://doi.org/10.1097/MD.00000000000016721>
- Gong Y, Chowdhury P, Nagesh PKB, Rahman MA, Zhi K, Yallapu MM, Kumar S (2020) Novel elvitegravir nanoformulation for drug delivery across the blood-brain barrier to achieve HIV-1 suppression in the CNS macrophages. *Sci Rep* 10:3835. <https://doi.org/10.1038/s41598-020-60684-1>
- Bruce RD, Katz EM, Kharasch ED, Moody DE, Morse GD (2006) Pharmacokinetic interactions between buprenorphine and antiretroviral medications. *Clin Infect Dis* 43:S216. <https://doi.org/10.1086/508186>
- Satpathy R, Ghosh S (2011) In-silico comparative study and quantitative structure-activity relationship analysis of some structural and physicochemical descriptors of elvitegravir analogs. *J Young Pharm* 3:246. <https://doi.org/10.4103/0975-1483.83776>
- Unger NR, Worley MV, Kisgen JJ, Sherman EM, Childs-Kean LM (2016) Elvitegravir for the treatment of HIV. *Expert Opin Pharmacother* 17:2359. <https://doi.org/10.1080/14656566.2016.1250885>
- Momper JD, Best BM, Wang J, Capparelli EV, Stek A, Barr E, Badell ML, Acosta EP, Purswani M, Smith E, Chakhtoura N, Park K, Burchett S, Shapiro DE, Mirochnick M (2018) IMPAACT P1026s protocol team. Elvitegravir/cobicistat pharmacokinetics in pregnant and postpartum women with HIV. *AIDS* 32:2507. <https://doi.org/10.1097/QAD.0000000000001992>
- (2016) Elvitegravir (Vitekta) for HIV *Med Lett Drugs Ther* 5:10–1. PMID: 26761343
- Prathipati PK, Mandal S, Destache C (2018) LC-MS/MS method for the simultaneous determination of tenofovir, emtricitabine, elvitegravir and rilpivirine in dried blood spots. *J Biomed Chromatogr* 26:e4270. <https://doi.org/10.1002/bmc.4270>
- Penchala SD, Fawcett S, Else L, Egan D, Amara A, Elliot E, Challenger E, Back D, Boffito M, Khoo S (2016) The development and application of a novel LC-MS/MS method for the measurement of Dolutegravir, Elvitegravir and Cobicistat in human plasma. *J Chromatogr B Anal Technol Biomed Life Sci* 1027:174. <https://doi.org/10.1016/j.jchromb.2016.05.040>
- Ocque AJ, Hagler CE, Morse GD, Letendre SL, Ma Q (2018) Development and validation of an LC-MS/MS assay for tenofovir and tenofovir alafenamide in human plasma and cerebrospinal fluid. *J Pharm Biomed Anal* 156:163. <https://doi.org/10.1016/j.jpba.2018.04.035>
- Simiele M, Ariaudo A, De Nicolò A, Favata F, Ferrante M, Carcieri C, Bonora S, Di Perri G, De Avolio A (2017) UPLC-MS/MS method for the simultaneous quantification of three new antiretroviral drugs, dolutegravir, elvitegravir and rilpivirine, and other thirteen antiretroviral agents plus cobicistat and ritonavir boosters in human plasma. *J Pharm Biomed Anal* 138:223. <https://doi.org/10.1016/j.jpba.2017.02.002>
- Bollen PDJ, De Graaff-Teulen MJA, Schalkwijk S, Van Erp NP, Burger DM (2019) Development and validation of an UPLC-MS/MS bioanalytical method for simultaneous quantification of the antiretroviral drugs dolutegravir, elvitegravir, raltegravir, nevirapine and etravirine in human plasma. *J Chromatogr B Anal Technol Biomed Life Sci* 1105:76. <https://doi.org/10.1016/j.jchromb.2018.12.008>
- Djerada Z, Feliu TC, Vautier D, Binet L, Robinet A, Marty H, Gozalo C, Lamiable D, Millart H (2013) Validation of a fast method for quantitative analysis of elvitegravir, raltegravir, maraviroc, etravirine, tenofovir, boceprevir and 10 other antiretroviral agents in human plasma samples with a new UPLC-MS/MS technology. *J Pharm Biomed Anal* 86:100. <https://doi.org/10.1016/j.jpba.2013.08.002>
- Sengupta P, Chatterjee B, Tekade RK (2018) Current regulatory requirements and practical approaches for stability analysis of pharmaceutical products: a comprehensive review. *Int J Pharm* 543:328. <https://doi.org/10.1016/j.ijpharm.2018.04.007>
- Yanagisawa K (2015) Transition of psychotropic drugs in Japanese pharmacopoeia (JP) (Part 15). Transitions in the standards and test methods of potassium bromide in JP I (1886) and JP X VI (2011), and Comparison between the USP and BP. *Yakushigaku Zasshi* 50:13
- Kameyama Y, Matsuhama M, Mizumaru C, Saito R, Ando T, Miyazaki S (2019) Comparative study of pharmacopoeias in Japan, Europe, and the United States: toward the further convergence of international pharmacopoeial standards. *Chem Pharm Bull (Tokyo)* 67:1301. <https://doi.org/10.1248/cpb.c19-00621>
- Reddy GM, Bhaskar BV, Reddy PP, Ashok S, Sudhakar P, Babu JM, Vyas K, Mukkanti K (2007) Structural identification and

- characterization of potential impurities of pantoprazole sodium. *J Pharm Biomed Anal* 45:201–210. <https://doi.org/10.1016/j.jpba.2007.05.032>
25. Bharathi Ch, Prasad ChS, Bharathi DV, Shankar R, Rao VJ, Dandala R, Naidu A (2007) Structural identification and characterization of impurities in ceftizoxime sodium. *J Pharm Biomed Anal* 43:733–740. <https://doi.org/10.1016/j.jpba.2006.07.031>
26. Maggio RM, Calvo NL, Vignaduzzo SE, Kaufman TS (2014) Pharmaceutical impurities and degradation products: uses and applications of NMR techniques. *J Pharma Biomed Anal* 101:102–122. <https://doi.org/10.1016/j.jpba.2014.04.016>
27. Thomas S, Paul SK, Shandilya S, Agarwal A, Saxena N, Awasthi AK, Matta HB, Vir D, Mathela CS (2012) Identification and structural elucidation of two process impurities and stress degradants in darifenacin hydrobromide active pharmaceutical ingredient by LC-ESI/MSn. *Analyst* 137:3571–3582. <https://doi.org/10.1039/C2AN35454C>
28. De Alvarenga Junior BR, Carneiro RL (2019) Chemometrics approaches in forced degradation studies of pharmaceutical drugs. *Molecules* 24:3804. <https://doi.org/10.3390/molecules24203804>
29. Shankar G, Borkar RM, Suresh U, Guntuku L, Naidu VGM, Nagesh N, Srinivas R (2017) Forced degradation studies of lansoprazole using LC-ESI HRMS and ¹H-NMR experiments: in vitro toxicity evaluation of major degradation products. *J Mass Spectrom* 52:459–471. <https://doi.org/10.1002/jms.3949>
30. Sambandan E, Kathavarayan T, Sellappan S, Shiea J, Ponnusamy VK (2019) Identification and characterization of unknown degradation impurities in beclomethasone dipropionate cream formulation using HPLC, ESI-MS and NMR. *J Pharm Biomed Anal* 167:123–131. <https://doi.org/10.1016/j.jpba.2019.02.013>
31. Zhao L, Wang Q, Bie Y, Lu X (2017) Isolation, identification and characterization of potential impurities of anidulafungin. *J Pharm Biomed Anal* 141:192–199. <https://doi.org/10.1016/j.jpba.2017.04.014>
32. Sahu PK, Ramiseti NR, Cecchi T, Swain S, Patro CS, Panda J (2018) An overview of experimental designs in HPLC method development and validation. *J Pharm Biomed Anal* 147: 590–611. <https://doi.org/10.1016/j.jpba.2017.05.006>
33. Arumugam A, Joshi A, Vasu KK (2017) Development and validation of a stability-indicating HPLC method for imidapril and its degradation products using a design of experiment (DoE) approach. *J AOAC Int* 100:1727–1738. <https://doi.org/10.5740/jaoacint.16-0329>
34. Vitekta EMA assessment report, EMA/701401/2013 (2013) https://www.ema.europa.eu/en/documents/assessment-report/vitekta-epar-public-assessment-report_en.pdf
35. ICH Q2 (R1), Validation of analytical procedures: text and methodology, 1995. <https://www.fda.gov/regulatory-information/search-fda-guidance-documents/q2-r1-validation-analytical-procedures-text-and-methodology/>. Accessed 20 April 2020
36. Patel VB, Patel AD, Shah DA (2018) Stability indicating liquid chromatographic method for simultaneous determination of aspirin and omeprazole. *Curr Drug DiscovTechnol* 15:351–360. <https://doi.org/10.2174/1570163814666171023144105>
37. Saini S, Sharma T, Patel A, Kaur R, Tripathi SK, Katare OP, Singh B (2020) QbD-steered development and validation of an RP-HPLC method for quantification of ferulic acid: rational application of chemometric tools. *J Chromatogr B: Analyt Technol Biomed Life Sci* 1155:122300. <https://doi.org/10.1016/j.jchromb.2020.122300>
38. Wiberg K, Andersson M, Hagman A, Jacobsson SP (2004) Peak purity determination with principal component analysis of high-performance liquid chromatography-diode array detection data. *J Chromatogr A* 1029:13–20. <https://doi.org/10.1016/j.chroma.2003.12.052>
39. Nikolin B, Imamović B, Medanhodžić-Vuk S, Sober M (2004) High performance liquid chromatography in pharmaceutical analyses. *Bosn J Basic Med Sci* 4:5–9. <https://doi.org/10.17305/bjbms.2004.3405>

Publisher's Note Springer Nature remains neutral with regard to jurisdictional claims in published maps and institutional affiliations.

Springer Nature or its licensor (e.g. a society or other partner) holds exclusive rights to this article under a publishing agreement with the author(s) or other rightsholder(s); author self-archiving of the accepted manuscript version of this article is solely governed by the terms of such publishing agreement and applicable law.